A Comprehensive Study on Adsorption Behaviour of Direct, Reactive and Acid Dyes on Crosslinked and Non-crosslinked Chitosan Beads

Chihim J Luk [a], Joanne Yip [a,*], Chunwah Marcus Yuen [a]
Chiwai Kan [a], Kimhung Lam [b]

[a]*Institute of Textiles and Clothing, The Hong Kong Polytechnic University, Hong Kong*
[b]*Applied Biology and Chemical Technology, The Hong Kong Polytechnic University, Hong Kong*

Abstract

Chitosan beads demonstrate good adsorption capacity in wastewater treatment. The ease with which the chitosan beads separate from the effluent and the possibilities of sorbent regeneration have made chitosan beads a more prominent form for biosorption. However, chitosan beads form gels at pHs below 5.5, which makes them unsuitable to be employed in treatment process. Bifunctional agents are introduced to increase the integrity of the beads by crosslinking chitosan. Crosslinked chitosan beads exhibit different adsorption capacities for distinct types and categories of dyestuffs. In this study, the removal of Direct Red 80 (DR80), Reactive Yellow 25 (RY25) and Acid Blue 25 (AB25) dyes by chitosan-based beads has been investigated. Variation in pH and temperature, effect of crosslinking and encapsulation of bacteria *Lactobacillus casei* are evaluated for their influence on the adsorption behaviour. Zeta potential and structural characterization of the synthesized chitosan beads are performed. Adsorption equilibriums are achieved in about five hours. The chitosan beads are crosslinked with glutaraldehyde to avoid their dissolution at pH 2 and the beads achieve complete removal of the three dyes within one hour. Temperature increase induces a positive effect on the adsorption of DR80, but an insignificant effect on that of RY25 and negative effect on AB25. Adsorption with the crosslinked beads at pH 5.5 and 37 °C promotes the removal of RY25 and AB25 by at least two folds more than that by non-crosslinked chitosan beads, but is found to be less effective on DR80. Significant increase of DR80 adsorption is achieved by adopting the crosslinked-bacteria-encapsulated chitosan beads while the effect on AB25 and RY25 are similar when compared to blank crosslinked beads. Langmuir and Freundlich isotherms fit the experimental data and the pseudo-second order equation agrees very well with the kinetic data.

Keywords: Chitosan Beads; *Lactobacillus Casei*; Dye Adsorption; Langmuir; Freundlich

---

*Corresponding author.
Email address:* `tcjyip@polyu.edu.hk` (Joanne Yip).

1 Introduction

Among the 0.7 million tons of dye produced worldwide, 5-10% comes from the textile industry and is discharged into waste streams annually [1]. Most of these dyes are synthetic dyestuffs which are highly visible in water even at low concentrations. This will significantly affect photosynthesis-related activity that relies on sunlight penetration. Proper treatment of textile effluent becomes environmentally important. Direct Red 80 (DR80), Reactive Yellow 25 (RY25) and Acid Blue 25 (AB25) are anionic dyes commonly used in textile industry. They produce strong colour intensities owing to their extensive chromophores, thereby influencing hydrosphere. They all possess sulfonate groups which contribute to efficient adsorption as far as ionic interaction with adsorbent is concerned, i.e. DR80, RY25 and AB25 have six, two and one sulfonate groups respectively. Moreover, the molecular mass of these three dyes are significantly different, i.e. DR80 1373.07 g·mol^{-1}; RY25 788.4 g·mol^{-1}; AB25 416.38 g·mol^{-1}. In order to investigate the influence of functional groups and molecule size on dye adsorption, these three dyes were chosen as the study model.

Conventional physical and chemical treatment techniques, including activated sludging, trickling filtering, chemical oxidation and coagulation, have been extensively studied to remove dyestuffs from water bodies [2]. However, the dyestuffs are usually recalcitrant molecules which are stable towards oxidation and resistant to biodegradation. Therefore, the sorption technique has been introduced and successfully employed for the removal of toxic dye molecules [3]. Although activated carbon is an effective sorbent in treating dye laden wastewater, the high cost and regeneration difficulties of the material make it unfavourable for commercial applications. Biosorbents, which are sorbents either as waste biomaterials or materials derived from bio-origins, have been investigated for colour removal by biosorption owing to their tonnage quantities and low cost. Some common biosorbents used for this purpose are peanut hulls [4, 5], fruit peels [6, 7] and rice husks [8, 9]. Moreover, different types of synthetic polymer are also evaluated as brilliant adsorbents, e.g. compounded polyethylene terephthalate with Boltorn H40 [10]. In particular, chitosan presents itself as an excellent biosorbent which can even achieve a higher dye removal capacity than activated carbon [11] with other beneficial terms such as natural abundance, biodegradability and low cost [12].

Chitosan, a deacetylated form of chitin, is a biopolymer of glucosamine which contains high contents of amine and hydroxyl functional groups. In acidic conditions, the amine groups of chitosan are protonated to electrostatically attract anionic dye molecules, thereby removing dye from an aqueous solution. When compared with chitosan flakes, chitosan beads demonstrate more superior adsorption capacity in wastewater treatment studies [13]. Besides that, the ease of separation of chitosan beads from effluent and the possibility of sorbent regeneration have made chitosan beads the more prominent form for biosorption. Nevertheless, chitosan beads form gels at pHs below 5.5, which makes them unsuitable to be employed in the treatment process. Bifunctional agents are introduced to increase the integrity of the beads by crosslinking the chitosan. Crosslinked chitosan beads exhibit different adsorption capacities for distinct types and categories of dyestuffs, and thus they are of interest for maintaining the integrity of the beads while maximizing their adsorption capacity.

In this study, the efficacy of the adsorption DR80, RY25 and AB25, by chitosan beads under different conditions is presented. The adsorption capacities of non-crosslinked, glutaraldehyde-crosslinked and *L. casei*-encapsulated chitosan beads are investigated. Since the adsorption capacity of anionic dyes in aqueous solutions is influenced by the pH, temperature of the bulk

solution and the nature of the employed adsorbent, adsorption of the three anionic dyes are evaluated as a function of these parameters. The Langmuir and Freundlich equations are employed to fit the equilibrium isotherms at pH 5.5 with various initial dye concentrations. The adsorption rate is quantitatively studied by the pseudo-first- and -second-order models. The experimental data indicate satisfactory performance of the chitosan beads under different conditions and their prominent potential to remove certain types of textile dyes.

2 Experimental

2.1 Chemicals

All chemicals were purchased from Sigma Aldrich Company Ltd.: chitosan (practical grade, from shrimp shells, $\geq 75\%$ deacetylated), glutaraldehyde (50% m/v aqueous solution), methanol (ACS grade), sodium hydroxide (NaOH), glacial acetic acid (CH_3COOH), potassium bromide (FT-IR grade), RY25, DR80, AB25, magnesium sulphate ($MgSO_4$), calcium chloride ($CaCl_2$), mono-potassium dihydrogen phosphate (KH_2PO_4), dipotassium hydrogen phosphate (K_2HPO_4), sodium chloride (NaCl), glucose, peptone, and yeast extract (for the bacterial culture).

2.2 Preparation of the Chitosan Beads

Chitosan (1.4% w/v) was dissolved in 1.4% acetic acid and stirred overnight. The chitosan solution was then centrifuged at 4 000 rpm for 10 min. The supernatant was used subsequently. 0.5 M Methanolic NaOH was prepared by dissolving NaOH pellets in deionized water and mixed with methanol in a volume ratio of 8:2. A syringe with a 25 G needle tip was used for the coacervation process. 10 mL of chitosan solution was pumped into 50 mL of methanolic NaOH by a syringe pump operated at 2 mL·min^{-1}. Chitosan beads were instantaneously formed in the constantly agitating alkaline medium. After stirring for 60 minutes, the chitosan beads were filtered and thoroughly washed with distilled water.

Glutaraldehyde is a bifunctional crosslinking agent which is capable of modifying the chitosan beads. The crosslinked chitosan beads were synthesized by mixing non-crosslinked chitosan beads with a glutaraldehyde solution (0.5% w/v) at room temperature for 15 minutes to allow a complete crosslink. The crosslinked chitosan beads were filtered out and washed with distilled water.

Besides chemical modification, biological modification of the chitosan beads with *Lactobacillus casei* (*L. casei*) was also adopted. Various researches have been done on the study of removal of synthetic dyes with single or mixed bacterial strain while immobilization of bacteria on biopolymer to remove dyes is still unexplored [14-16].

The *L. casei* cultural medium was prepared according to the following composition (g·L^{-1}): $MgSO_4$ (0.2), $CaCl_2$ (0.04), KH_2PO_4 (1.0), K_2HPO_4 (1.0), NaCl (0.04), glucose (1.0), peptone (1.0) and yeast extract (0.5). Freshly prepared cultural medium (100 mL) was incubated at 37 °C on a rotatory shaker (250 rpm) for 1 hour. Freshly available Yakult (1 mL) was transferred into the medium and incubation was continued. At the 31st hour, the culture was withdrawn and the cell pellet was obtained upon centrifugation at 4, 000 rpm for 20 min. The supernatant was discarded and the tube of bacterial cells was freeze-dried overnight. The *L. casei*-encapsulated chitosan beads were synthesized by similar procedures as the non-crosslinked chitosan beads.

Dried *L. casei* was mixed well with chitosan solution at 11.5 mg·mL^{-1}and then followed by the alkaline hardening process.

All beads were stored in distilled water after filtration and washing. Before the experiment, the surface moisture of the beads was removed by filter paper. The particle diameter of the non-crosslinked and crosslinked chitosan beads was determined by a ruler with the aid of a magnifying glass as 3.0 mm and 2.5 mm, respectively [17].

2.3 FTIR Spectroscopy

Fourier Transform Infrared (FTIR) spectra of glutaraldehyde-crosslinked and non-crosslinked chitosan beads were obtained by a Perkin-Elmer Spectrum 100 FT-IR spectrometer. Dried-pressed pellets were obtained by grinding different samples with FTIR grade KBr on an agate mortar followed by drying in the oven.

2.4 Zeta Potential Measurement

Non-crosslinked and glutaraldehyde-crosslinked chitosan beads were dried (equivalent to 100 mg dried mass), ground and mixed with 100 mL of deionized water respectively. The mixtures were sonicated for 4 hours, and then stirred for 24 hours. The suspensions were subjected to Zeta potential measurement with a ZetaPlus Zeta potential analyser (BrookHarven Instrument Co.). Before the measurement, the suspensions were withdrawn into different vials and pre-assigned pH values were adjusted by various concentrations of HNO$_3$ and NaOH solutions respectively without addition of background electrolytes.

2.5 Adsorption Experiments

Buffered solutions with pH values of 2, 3.4, 4.6 and 5.5 were used. The adsorption experiments with blank chitosan beads were performed by batch procedures at temperatures of 25 °C, 37 °C and 50 °C using 100 mg·L^{-1} aqueous dye solution. In each adsorption experiment, 3 g blank chitosan beads (crosslinked chitosan beads in dye solution at pH 2) were added to 50 mL of dye solution with known concentration in a 50 mL conical tube. The tube was continuously shaken at 200 rpm at the temperatures described above. Aliquot samples were taken at a predetermined time interval and the dye concentration was spectrophotometrically measured at 421, 528 and 574 nm for the RY25, DR80 and AB25 dyes respectively by a Perkin-Elmer Lambda 18 UV-VIS spectrophotometer.

The adsorption experiments with the dried *L. casei* encapsulated chitosan beads were carried out at 37 °C with a pH 5.5 medium. The operating procedures were the same as those described above.

The decolourization efficiency was calculated by the following expression:

$$Q = \frac{C_0 - C}{C_0} \times 100\% \tag{1}$$

where Q is the decolourization efficiency, C_0 is the initial concentration of the dye solution (mg·L^{-1}) and C is the concentration of dye present at a predetermined time.

2.6   Kinetics

Kinetic experiments were performed by mixing 3 g of chitosan adsorbent with 50 mL of dye solution (100 mg·L^{-1}). The suspension was shaken for 5 hours at pHs 3.4, 4.6 and 5.5 for all three dyes in an incubator at 37 °C. At regular intervals, the concentration of the dye in the solution was determined.

2.7   Equilibrium Adsorption Isotherm

The effect of the initial dye concentration was determined by mixing 3 g of chitosan adsorbent with 50 mL of dye solution at different initial concentrations (0-200 mg L^{-1}). The suspension was shaken for 24 hours at pH 5.5 for all three dyes in an incubator at 37 °C.

3   Results and Discussion

3.1   FTIR Spectroscopy

Fig. 1 (a) and 1 (b) show the FTIR spectra of non-crosslinked and crosslinked chitosan beads, respectively. In Fig. 1 (a), the absorption at 1640.9 cm^{-1} is caused by the N-H bending of the primary amine and 1087.9 cm^{-1} is caused by C-N stretching. In Fig. 1 (b), the absorption band at 1663.8 cm^{-1} is attributed to the C═N bonding formed through crosslinking with glutaraldehyde and the absorption at 1566.4 cm^{-1} is due to the N-H bending of the amide which is presented as a result of incomplete deacetylation of the chitosan. Besides the corresponding characteristic absorption peaks, other common peaks are observed from the two spectra, including the O—H stretching near 3433 cm^{-1}, the C—H stretching of sp^3 carbon near 2900 cm^{-1}, and the C—O—C stretching of ether around 1377 cm^{-1} [18, 19].
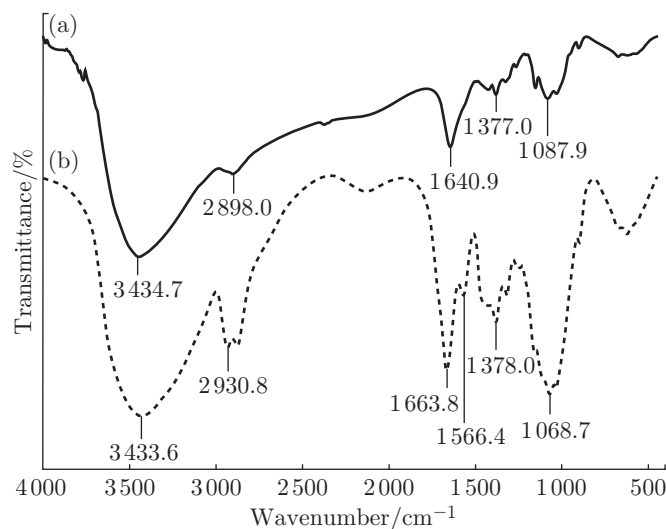
Fig. 1: FTIR spectrum of (a) Non-crosslinked and (b) Crosslinked chitosan beads

3.2   Zeta Potential Measurement

Adsorption of anionic dyes onto chitosan beads depends on the surface charge of the adsorbent at different bulk pHs [3]. The three anionic dyes chosen in this study have different numbers of —SO_3^- groups. On the other hand, chitosan has numerous —NH_2 and —OH groups which contribute different surface charges upon protonation or vice versa under acidic and alkaline mediums respectively. Hence, anionic dyes and chitosan would have different extents of electrostatic interaction under different pH environments. The Zeta potentials of non-crosslinked and crosslinked chitosan beads which were measured ranged from pH 3-12 and are shown in Fig. 2. The overall Zeta potentials of both beads are positive in an acidic medium and negative after pH 8. An isoelectric point was reached at around pH 8 for both beads, where the surface charge of the beads was neutral. The Zeta potentials of non-crosslinked beads before the isoelectric point were more positive than those of crosslinked beads. This could be attributed to the protonation of the amine group (R—NH_2) on chitosan into the corresponding ionic form (R—NH_3^+). Availability of the primary amine group on chitosan was reduced which were converted to imide (R—C$=\!=$N) after crosslinking. Relatively more protonation of non-crosslinked beads hence gave more positive Zeta potentials in the acidic medium. The positive surface charge of both beads in the acidic medium was helpful for interpreting particular adsorption performances of anionic dyes in that the positively charged bead surfaces could adsorb dyes by counter ionic attraction. Vice versa, negative Zeta potentials were demonstrated beyond the isoelectric point which was possibly due to the surface interaction with OH^- ions.
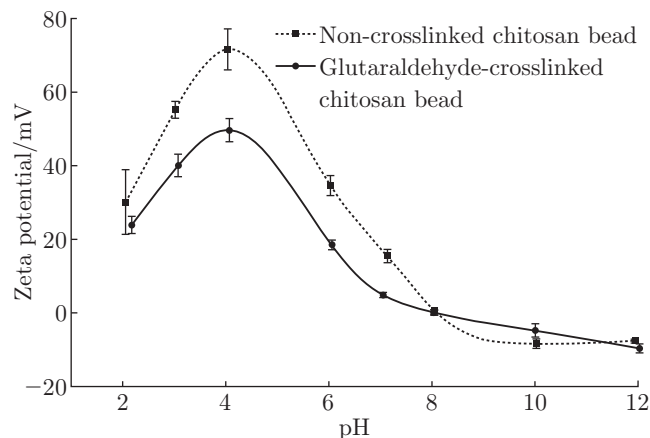
Fig. 2: Zeta potentials of non-crosslinked and glutaraldehyde-crosslinked chitosan beads

3.3   Effect of pH

Fig. 3 shows the effect of pH on the adsorption of the three different dyes. Maximum uptake for all three dyes is observed at pH 2 which is in accordance with the studies of Chiou and Li [3], who investigated the adsorption of Reactive Red 189 with crosslinked chitosan beads, and Kyzas and Lazaridis [11] who performed adsorption of Remazol Yellow Gelb 3RS onto chitosan derivatives. The high percentage removal of the three anionic dyes could be attributed to the electrostatic interaction between the protonated amino groups (R—NH_3^+) of the chitosan beads and the anionic groups (D—SO_3^-) of the dye molecules formed through dissociation under acidic

conditions according to the following reaction [20].

$$R\text{—}NH_2 + H_3O^+ \rightarrow R\text{—}NH_3^+ + H_2O \tag{2}$$

$$D\text{—}SO_3Na \rightarrow D\text{—}SO_3^- + Na^+ \tag{3}$$
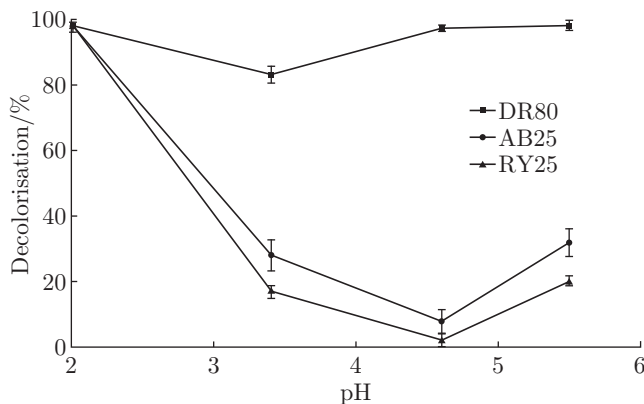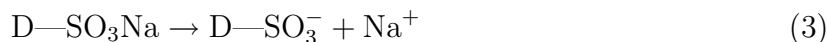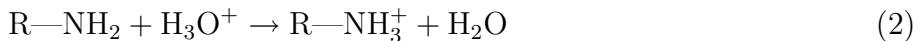
Fig. 3: Effect of pH on the decolourization efficiency of 100 mg/L solution of DR80, RY25 and AB25 at 37 °C

The adsorption proceeds through the interaction of the counter ions:

$$R\text{—}NH_3^+ + {}^-O_3S\text{—}D \rightarrow R\text{—}NH_3^+ \cdots {}^-O_3S\text{—}D \tag{4}$$

These interactions were consistent with the measurement outcome of the Zeta potential. Reactions (2) and (3) were achieved under acidic environment, where the beads had a positive surface charge. This allowed the formation of the chitosan-dye moiety (4), thus revealing that the removal mechanism mainly depended on the electrostatic interaction between the positively charged bead surface and the negatively charged SO_3^- group of the dyes.

Adsorption of the DR80 at all pH levels resulted in more than 90% dye removal. This could be explained by the multiple functional groups on the dye molecules resulting in the facilitation of dye adsorption onto the chitosan beads even when the number of protonated amino groups available decreased with increasing pH. However, there was a significant decrement in the decolouration percentage of AB25 and RY25 when the pH was increased beyond 2. This was due to the chemical structure of the dye molecules. AB25 showed a relatively higher adsorption with the chitosan beads as compared to that of RY25. The number of SO_3^- functional groups present in both dyes was the same. RY25 has a comparatively bulkier structure than AB25. Accordingly, the adsorption of RY25 molecules into the bulk solution might be hindered by the already-adsorbed-RY25 molecules on the chitosan bead surface. This resulted in a lower adsorption percentage of RY25 following the adsorption mechanism. Although AB25 molecules have a ramified structure which prevents them from removal by diffusion mechanisms, yet the less bulky structure of the dye molecules could lessen the steric hindrance of subsequent dye molecule adsorption. As a result, the AB25 dye showed a higher percentage of decolouration than RY25 at all pH levels.

Nevertheless, it is worth noting the slight increase of adsorption of RY25 and AB25 at pH 5.5. With an increased solution pH, the surface charge became less positive. The increased adsorption of RY25 might occur through other interactions, such as Van der Waals forces or hydrogen bonding [21]. The hydroxyl groups of chitosan can be deprotonated under alkaline conditions as follows:

$$\text{—}CH_2\text{—}OH + OH^- \rightarrow \text{—}CH_2O^- + H_2O \tag{5}$$
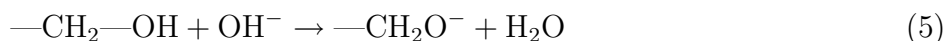
Thus bonding was formed between the dissociated anionic-CH_2O^- group and RY25 molecules through substitution of the Cl^-group in the dye [22]:

$$—CH_2O^- + Dye - Cl \rightarrow —CH_2—O\text{-Dye} + Cl^- \tag{6}$$
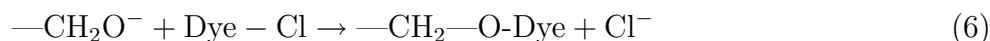
3.4   Effect of Temperature

Fig. 4 shows the temperature effect on the adsorption of the three dyes. At the end of 300 min, DR80 shows the highest dye removal at any temperature when compared to AB25 and RY25. It was assumed that all the anionic dyes would be basically adsorbed by the negatively charged SO_3^- groups of the dye molecules through the surface adsorption mechanism. In the case of DR80, an increase in temperature led to an enhancement of the initial adsorption rate while the adsorption capacity at the fifth hour was similar. As shown in Fig. 4 (a), the initial adsorption rate of DR80 at 50 °C is the highest among the three temperatures. Nevertheless, the equilibrium adsorption amounts were about 86% for all three temperatures. A similar trend was observed in the study on DR80 by Saleem *et al.* [23]. The increase in the dye adsorption rate with respect to temperature indicates that the adsorption of the DR80 dye is a kinetic controlling and endothermic process. Besides, with the large amount of functional groups per molecule on DR80, it was also proposed that some branches of the molecules might be able to bind with the protonated amino groups in the inner surface of the chitosan beads due to the enlargement of the chitosan bead pores
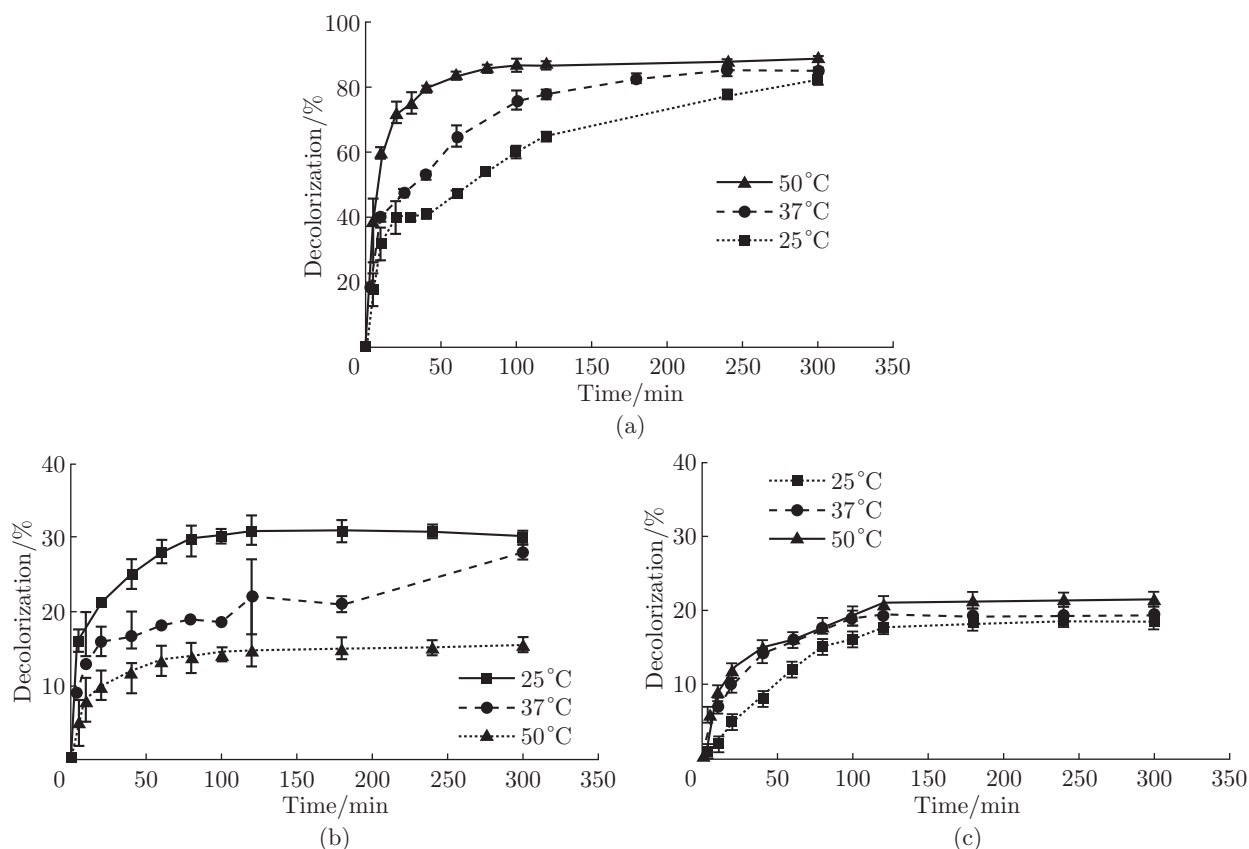
Fig. 4: Effect of temperature on the adsorption of (a) DR80, (b) AB25 and (c) RY25 at 25 °C, 37 °C and 50 °C

caused by the increased temperature [24]. According to Mazengarb and Roberts [25], direct dyes can diffuse into chitosan films during the adsorption process due to the amorphous nature of the chitosan film and the diffusion coefficient of the dye which decreases with temperature. It can therefore explain the higher removal percentage of the DR80 dye with increased diffusion rate into the enlarged chitosan pores at higher temperatures in the adsorption process and vice versa. As for the removal of AB25 and RY25, the temperature effect was comparatively insignificant. The adsorption kinetics of the RY25 dye at all temperatures was found to be similar to a maximum adsorption capacity of around 20%. The maximum amount of removal of the AB25 dye is higher than that of the RY25 dye which achieved a value of about 30%. The reason for the higher adsorption capacity is due to the less bulky structure of AB25 which enhanced the adsorption of dye molecules from the bulk solution. Both the initial rate and equilibrium removal amount of AB25 dye as shown in Fig. 4 (b) were slightly decreased by increasing the temperature from 25 °C to 50 °C. This suggests that the adsorption of AB25 is relatively exothermic and involves a physical process [26]. It can also be attributed to the ramified dye structure with only one adsorption site per molecule. Furthermore, according to Prado *et al.* [27], the intramolecular interaction between the —SO_3^- and the —NH_2 groups of the dye molecule, which are *ortho* to each other, also diminishes the effectiveness of the —SO_3^-—NH_3^+ interaction between the dye and chitosan to give reduced decolourization .

3.5   Effect of Crosslinking

The removal of DR80 could be as high as 95%, i.e. 32.2 mg·g^{-1} adsorbent, while that of RY25 was around 20% using non-crosslinked beads. Nevertheless, with the use of the crosslinked chitosan beads, the removal of RY25 is increased to more than 70% while that of DR80 drastically drops down to less than 40% as shown in Fig. 5. This shows the effect of crosslinking the chitosan beads on dye removal and the close relationship between the removal mechanisms and the structure of the dye molecules. As mentioned in the previous section, the removal of DR80 mainly follows the surface adsorption while some of the chain ends of the dye molecules may possibly bind with the protonated amino groups located in the inner surface of the chitosan bead pores. The removal of DR80 was significantly affected by the incorporation of the crosslinking agent since the average pore size of the chitosan beads was reduced by crosslinking the amine groups of the chitosan beads. Reduction in pore size reduces the possibility of long, branched dye molecules to have the —SO_3^- groups bind onto the bead inner pores, therefore greatly decreasing the surface area for the attachment of dye molecules, which resulted in over 50% reduction in the removal capacity of the dye. Moreover, the reduced number of protonable amino groups due to crosslinking as shown in Fig. 6 was also an additional factor which resulted in a drastic decrease in the removal of the DR80 dye. The adsorption capacities of RY25 and AB25 were increased through the crosslinking of the chitosan beads as they completely depend on surface adsorption for dye removal. Hence, the crosslinking of the chitosan beads resulted in an increased surface area due to a decreased bead size for the attachment of dye molecules. When compared with AB25, the removal of RY25 was much more prominent when using crosslinked chitosan beads to achieve 25.5 mg·g^{-1} adsorption. This can be explained by the Cl$^-$ group via a substitution removal mechanism which is only adopted by RY25. However, adsorption of AB25 could only be carried out by electrostatic attraction with a reduced number of protonable amino groups of the chitosan beads. In addition, this low level of AB25 removal (10.4 mg·g^{-1}) might also be attributed to the intramolecular structural effect between the —SO_3^- and the —NH_2 groups on the dye molecules. This clearly demonstrates that

a substantial effect could be brought by the differences in the interaction mechanism between the dye molecules and the adsorbent. Hence, it is important to lucidly understand the structure and properties of dyes before finding suitable and efficient adsorbents for the dye adsorption process.
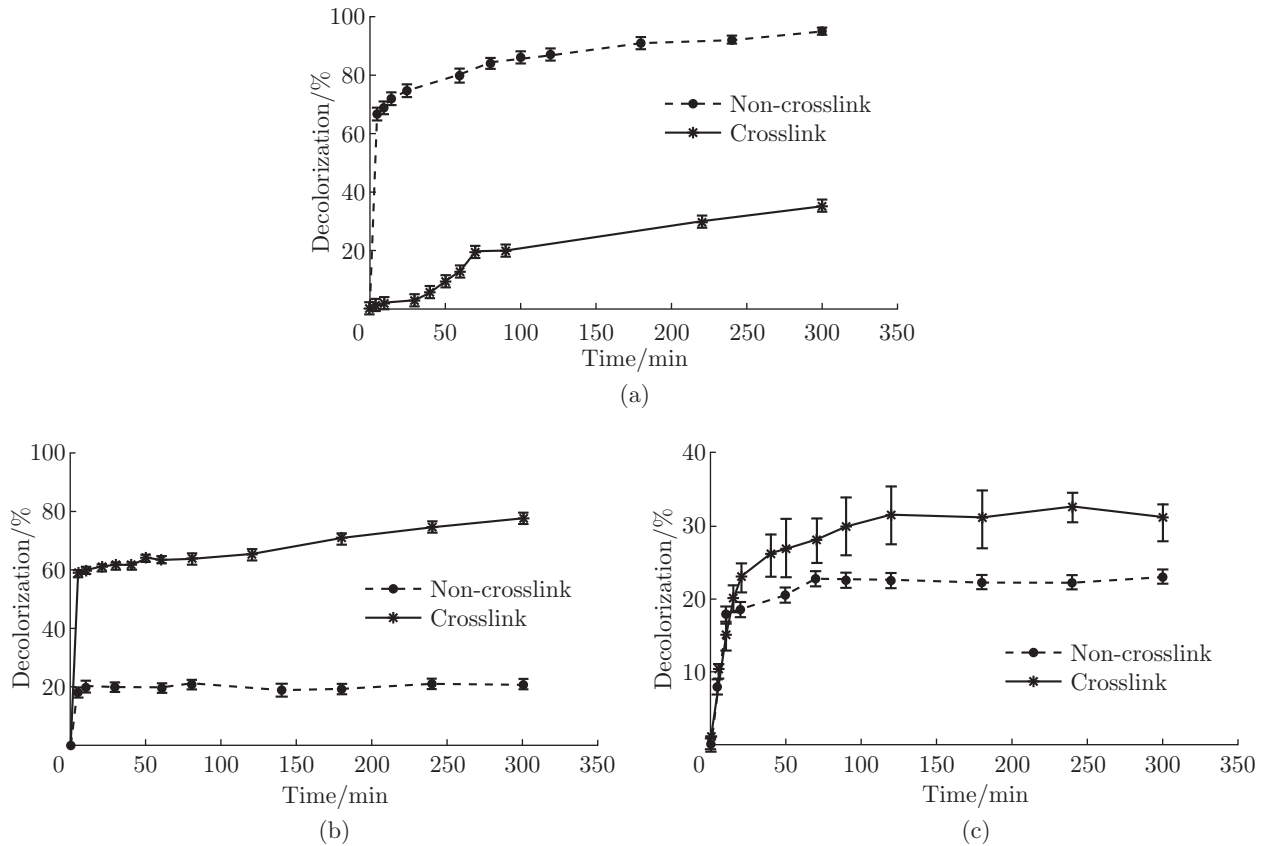
Fig. 5: Effect of crosslinking agent on the adsorption of (a) DR80, (b) RY25, and (c) AB25 using crosslinked and non-crosslinked chitosan beads
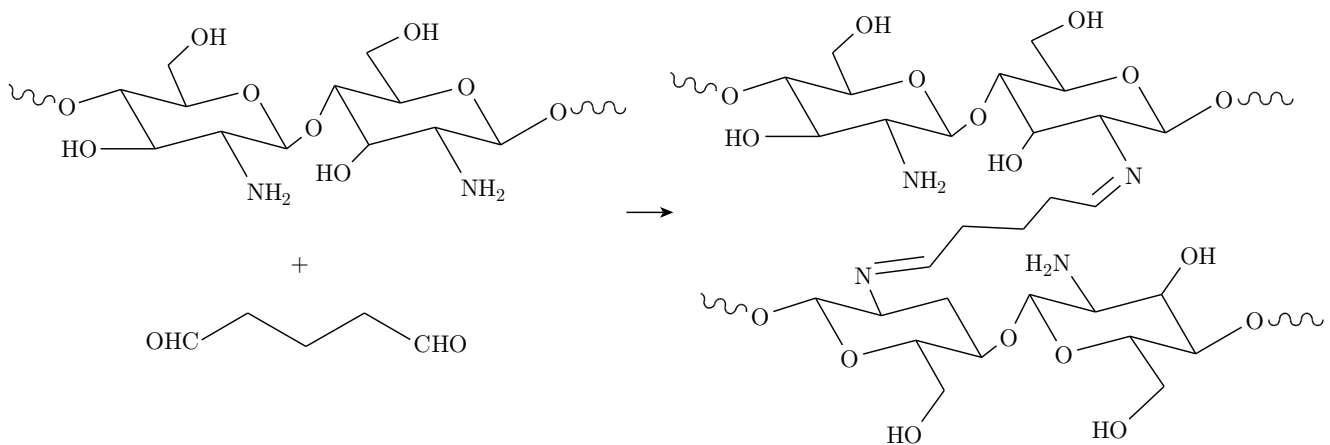
Fig. 6: Schematic diagram of glutaraldehyde crosslink on chitosan

3.6   Effect of Encapsulation of Dried L. Casei on Adsorption of Dyes

L. casei was encapsulated in crosslinked chitosan beads and studied for dye adsorption capacity. Fig. 7 depicts the dye removal efficiency with the bacteria encapsulated in the chitosan beads. Crosslinked beads without bacteria only remove about 33% of the DR80 while those that contain the bacteria achieve 80% decolourization. The crosslinked beads have a reduced pore size which prevents the diffusion of the dye molecules into the inner part of the beads. With the presence of the bacteria, additional biosorption sites are provided so that the binding of the dye molecules onto these various functional groups become possible thereby increasing the adsorption capacity. Apart from that, the DR80 removal capacity of *L. casei*-encapsulated-non-crosslinked chitosan beads could attain a rate that is higher than 80%. This reveals that crosslinking drastically reduces the removal efficiency of the DR80 when the pore size is reduced therefore decreasing the percentage of dye removal. However, the maximum percentage of adsorption within the incubation time for bacteria-encapsulated chitosan beads was around 80% for both non-crosslinked- and crosslinked-beads, which is still lower than that of the blank non-crosslinked chitosan beads i.e. about 93%. This once again demonstrates the adoption of the diffusion mechanism in addition to surface adsorption by DR80 which would be much refrained when the pore size is reduced or blocked by the encapsulated bacteria. On the other hand, encapsulation of *L. casei* could promote the removal efficiency of AB25 by about 10%. With the incorporation of the bacteria, an
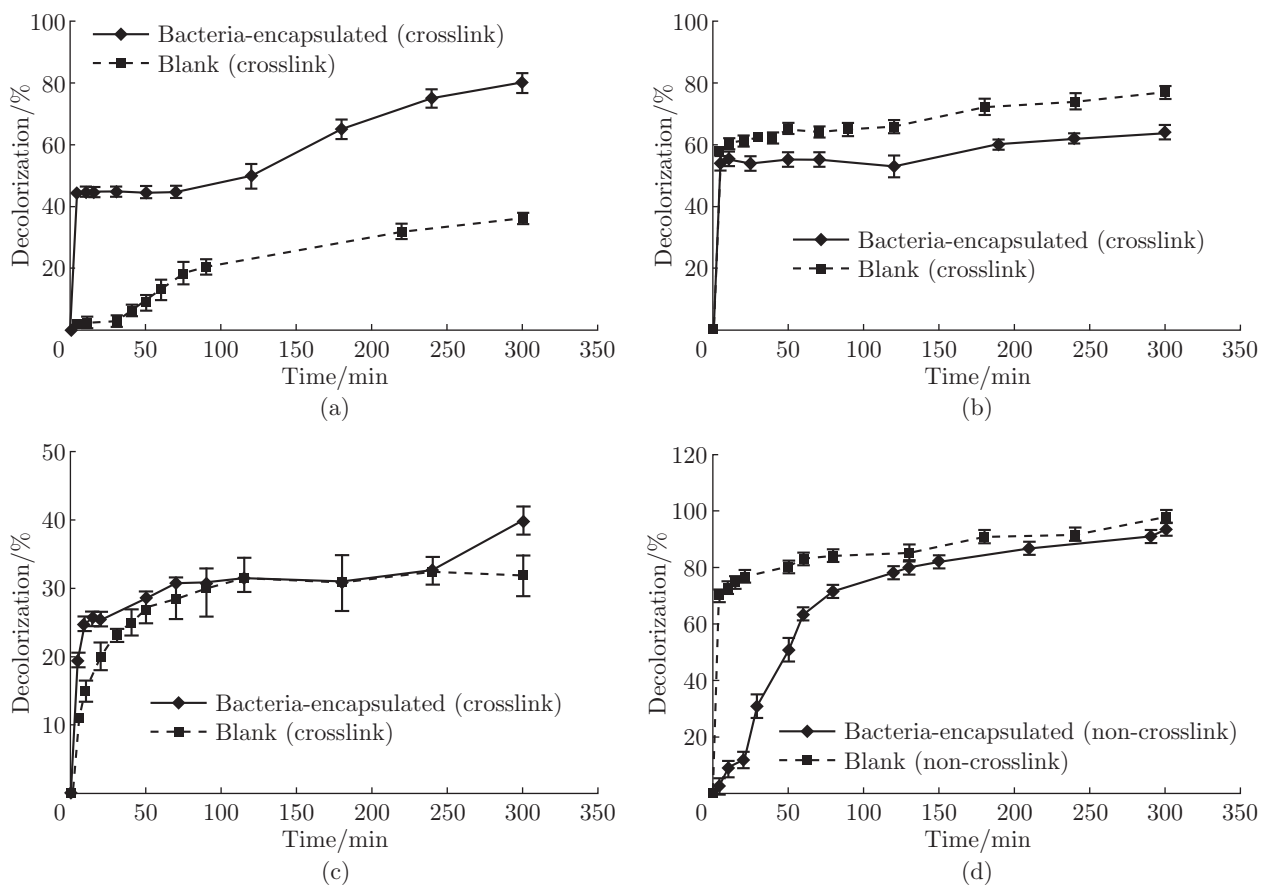
Fig. 7: Effect of bacteria encapsulation on the adsorption of (a) DR80, (b) RY25, (c) AB25 by crosslinked chitosan beads, and (d) DR80 by non-crosslinked beads, with bacteria-encapsulated and blank chitosan beads

increased number of interactions between the adsorption sites and dye molecules counterbalance the negative effect brought about by fewer amino sites through crosslinking. It is also possible that the various functional groups of the bacteria could hold the dye molecules in a tighter way which strengthened the counterbalancing effect.

Nevertheless, it was observed that the encapsulation of *L. casei* in crosslinked chitosan beads decreases the percentage removal of RY25 to about 65% when compared to that of the blank crosslinked chitosan beads which is more than 75%. This phenomenon is attributed to the binding interaction of the bacteria with the hydroxyl group on the chitosan which leads to a reduced number of available —CH_2O^- groups for dye substitution.

3.7   Adsorption Kinetics

To determine the mechanism of adsorption, kinetic data used for the removal of the three anionic dyes at the respective pH were correlated with the linear forms of the pseudo-first-order rate model,

$$\log(q_e - q) = \log q_e - \frac{k_1}{2.303}t \tag{7}$$

and the pseudo-second-order rate model,

$$\frac{t}{q} = \frac{1}{q_e}t + \frac{1}{k_2 q_e^2} \tag{8}$$

where q_e is the amount of adsorbed dye on the adsorbent (g·kg^{-1}) at equilibrium, q is the amount of adsorbed dye on the adsorbent (g·kg^{-1}) at time t, k_1 is the first-order adsorption rate constant (min^{-1}), and k_2 is the second -order adsorption rate constant (kg·g^{-1}min^{-1})

It has been suggested that the first order model does not fit well with the whole range of contact time in the adsorption experiments [25]. The results obtained in the present study are found to follow the same trend with the kinetic parameters which show a good adjustment to the pseudo-second-order model. Straight lines were plotted by correlating the adsorption data at all levels of pH to the pseudo-second-order model with high correlation coefficients, i.e. 0.9896 for DR80, 0.9590 for RY25, and 0.9545 for AB25 as shown in Table 1. This indicates that the adsorption system predominantly follows the pseudo-second-order model, and the rate controlling step of the overall process appears to be chemisorption instead of a mass transport mechanism. On the other hand, the high degree of non-linearity suggests the inability of the pseudo-first-order model to interpret relevant data [3, 28]. The pseudo-second-order model has been successfully applied to fit the kinetic data of: eosin Y by the chitosan hydrobeads [2], Reactive Red189 by the crosslinked chitosan beads [28], and Remazol Yellow Gelb 3RS and Basic Yellow 37 by the chitosan derivatives [12].

3.8   Equilibrium Adsorption Isotherm

The adsorption isotherms of DR80, RY25 and AB25 at pH 5.5 and 37 °C using the crosslinked beads were compared with the Freundlich and Langmuir isotherm models. The equilibrium adsorption capacity increases with an increase in dye concentration that ranged from 0-200 mg·L^{-1}. The two isotherm models introduced about 90 years ago still remain as the two most well known

Table 1: Kinetic constants for the adsorption of DR80, RY25 and AB25 by the chitosan beads

pH	DR80		RY25		AB25	
	k_2 (kg·g^{-1}min^{-1})	R^2	k_2 (kg·g^{-1}min^{-1})	R^2	k_2 (kg·g^{-1}min^{-1})	R^2
3.4	1.74×10^{-3}	0.999	0.02	0.959	4.95×10^{-3}	0.955
4.6	3.03×10^{-3}	0.998	0.01	0.964	–	–
5.5	4.39×10^{-3}	0.998	0.01	0.991	0.02	0.998

and commonly employed isotherm equations [12]. The Langmuir isotherm assumes the adsorbed layer of the adsorbent as a homogeneous mono-layer in nature. The expression of the Langmuir isotherm is given by:

$$\frac{C_e}{q_e} = C_e \left(\frac{1}{Q_{max}} \right) + \frac{1}{(Q_{max})K_L} \qquad (9)$$

where Q_{max} (mg·g^{-1}) is the maximum amount of dye adsorbed for a formation of monomolecular layer per unit weight of chitosan beads at equilibrium; C_e (mg·L^{-1}) is the equilibrium dye concentration; q_e (mg·g^{-1}) is the amount of dye adsorbed per unit mass of chitosan adsorbent at equilibrium; and K_L (L·mg^{-1}) is the Langmuir constant related to the affinity of the binding sites.

On the other hand, the Freundlich isotherm model interprets the adsorption that occurs on the adsorbent surface in a heterogeneous manner with uniform energy. The Freundlich equation can be expressed by:

$$\ln q_e = (\ln C_e)\frac{1}{n} + \ln K_F \qquad (10)$$

where q_e (mg·g^{-1}) is the amount of dye adsorbed per unit mass of chitosan adsorbent at equilibrium; C_e (mg·L^{-1}) is the equilibrium dye concentration; K_F is the Freundlich constant, which represents the adsorption capacity; and $(1/n)$ is the adsorption intensity [29].

The fitting parameters of the two models are computed in Table 2. The relatively low correlation coefficients show that the Langmuir isotherm has a poor agreement with the experimental data which suggests that the adsorption process of the present study does not occur on a single surface. On the contrary, the Freundlich isotherm fits the experimental data quite well with the high correlation coefficients, thus confirming the goodness of fitting i.e. $R^2 > 0.9888$ for all three anionic dyes. The consistency of the Freundlich isotherm with the data reveals that adsorption might occur in the heterogeneous adsorption sites. In addition, the interaction between the dye molecules and chitosan adsorbent could also vary according to the protonation equilibrium of different dyes [30]. Since this isotherm does not predict any saturation on the adsorbent surface, it thus shows the existence of physisorption and the occurrence of infinite surface coverage [12]. Although the experimental data do not fit the Langmuir isotherm well, yet the Q value that represents the maximum dye adsorption by the monolayer reflects the ease of the removal of DR80 which is more than RY25 and AB25 almost twofold and more than a hundred times the rate respectively. As a matter of fact, the protonation of the amino groups of chitosan would not be as effective as that under a pH 5.5 environment. As previously mentioned, the crosslinking of chitosan beads reduces the number of available protonated amino groups for surface

adsorption. Hence, the relatively high removal of DR80 could be due to a much higher number of $-SO_3^-$ functional groups possessed by each dye molecule. RY25 could be either adsorbed through electrostatic attraction of a single $-SO_3^-$ group per dye molecule or removed through the substitution mechanism of the $-Cl^-$ group.

Although there is a decrease in protonated amino groups with the increased surface area of the crosslinked chitosan beads, the adsorption of RY25 could still achieve a relatively high value when compared with the adsorption of the ramified AB25. The reduced number of protonable amino groups of the crosslinked chitosan beads accounts for the overall low adsorption of AB25, and at the same time, its intermolecular structural effect also attributes to poor adsorption capacity. Other than these factors, the $Q_{\max}$ of Langmuir isotherm and K_F of Freundlich model in mmol·g^{-1} are also included in Table 2. This shows that the isotherm constants are of reverse order when compared to the constants in mg·g^{-1}, i.e. AB25 has the largest value while DR80 has the smallest. This is attributed to the different molecular masses of these three dyes. From the viewpoint of mole, the actual amount of each adsorbate depends on the molecular mass when the same weight of dye is dissolved. Since the molecular masses of these three dyes are of descending order, i.e. from DR80 to RY25 and then to AB25, thus the number of mole in the solution during adsorption is in reverse order. As a result, when the isotherm model is interpreted in mmol·g^{-1}, it gives different outcome. It is worth to consider whether molar or mass quantity is more appropriate when studying particular adsorption. In the present study, weight quantity has been chosen in order to have a clear picture of practical water treatment. Besides the isotherm modelling, Table 3 lists some examples of dye adsorption with other adsorbents as a comparison to the present work [31-40].

Table 2: Adsorption isotherm parameters of DR80, RY25 and AB25 by the crosslinked chitosan beads

		DR80	RY25	AB25
Langmuir	$Q_{\max}$ (mg·g^{-1})	610.5	368.3	443.3
	$Q_{\max}$ (mmol·g^{-1})	0.4446	0.4671	1.065
	K_L (L·mg^{-1})	0.0049	0.0079	0.0827
	R^2	0.9105	0.8973	0.9233
Freundlich	K_F (mg·g^{-1})	0.3856	0.5563	0.3656
	K_F (mmol·g^{-1})	0.00028	0.00071	0.00088
	n	1.050	1.374	1.035
	R^2	0.9998	0.9987	0.9888

4   Conclusions

This study has investigated the dynamic adsorption of three types of anionic dyes, namely, DR80, RY25, AB25, on chitosan beads. The size of the non-crosslinked chitosan beads is about 3.0 mm in diameter while that of the crosslinked chitosan beads with 0.5 wt% glutaraldehyde is characterized to be about 2.5 mm. The crosslinked chitosan beads exhibit an extremely high adsorption capacity of 98% for removing all three anionic dyes at pH 2 and 37 °C. Adsorption using non-crosslinked chitosan beads reveals the ease of removal of the distinct dye at pH 3.4, 4.6 and 5.5 with DR80 being the easiest to remove, followed by AB25 and RY25 which are less

Table 3: Examples of dye adsorption on different adsorbents

Adsorbents	Target dyes	Adsorption capacity (Langmuir isotherm, mg·g^{-1})
Primary-secondary amino silica nanoparticle [31]	Direct red 80	41.2
	Direct Red 31	115
	Direct Black 22	37.5
	Acid Blue 92	114
Modified Multi-walled carbon nanotubes [32]	Direct red 23	189
	Direct red 80	121
Polyurethane foam [33]	Direct Red 80	4.50
	Recactive Blue 21	8.31
Mentha pulegium [34]	Direct red 80	52.4
	Acid Black 26	46.3
Potamogeton pusillus Ceratophylum demersum [35]	Acid Blue 25	184
		130
Amine-functionalized magnetic ferrite nanoparticle [36]	Direct red 31	186
	Acid Blue 25	161
	Acid red 14	147
Carya illinoinensis [37]	Acid Blue 74	13.4
	Acid Blue 25	4.85
	Reactive Blue 4	7.91
Natural sepiolite [38]	Acid blue 25	53.8
	Methylene Blue	78.4
Stoechospermum marginatum [39]	Acid Blue 25	40.0
	Acid Orange 7	67.1
	Acid Black 1	27.4
Base treated *Shorea dasyphylla* (sawdust) [40]	Acid Blue 25	24.4

easier to do so. The removal of the dye does not decrease with increasing pH which candidly illustrates that the mechanism of dye adsorption is closely related to the dye structure. Hence, the kinds of removal mechanisms adopted might sometimes outbalance the predicted mechanism i.e. electrostatic attraction between protonated amino groups of chitosan beads and anionic dye molecules. The present study has successfully revealed the behaviour of different types of anionic dyes and their dependence on the respective adsorption mechanism that corresponds to their chemical structure. The pseudo-second-order kinetic model successfully fits the adsorption behaviour of the three anionic dyes at different pH values, which indicates that the overall dye removal processes are chemisorption-controlled. The temperature effect on RY25 and AB25 is not significant. However, the adsorption of DR80 shows a higher rate with an increase in temperature which is probably due to the diffusion capability of the long-chain branched structure of the dye

molecules. The incorporation of a hardening agent, i.e. 0.5 wt% glutaraldehyde, affects the adsorption capacity of DR80 in a drastic manner. On the contrary, maximum enhancement in the adsorption capacities of RY80 and AB25 is due to an increase in the total surface area for dye adsorption. Encapsulation of *L. casei* into the chitosan beads encourages the adsorption of DR80 and AB25 while depressing the removal of RY25. The entrapment of bacteria strain into crosslinked chitosan beads showed different degree of affinity towards different dye classes. The Freundlich isotherm model agrees very well with the equilibrium adsorption data at different initial concentrations of the three anionic dyes.

Acknowledgements

References

[1] Wong Y, Yu J. Laccase-Catalyzed Decolorization of Synthetic Dyes. Water Res: 1999; 33: 3512-3520.

[2] Chatterjee S, Chatterjee S, Chatterjee BP, Das AR, Guha AK. Adsorption of a Model Anionic Dye, Eosin Y, from Aqueous Solution by Chitosan Hydrobeads. J Colloid Interface Sci: 2005; 288: 30-35.

[3] Chiou MS, Ho PY, Li HY. Adsorption of Anionic Dyes in Acid Solutions using Chemically Cross-Linked Chitosan Beads. Dyes Pigments: 2004; 60: 69-84.

[4] Tanyildizi MS. Modeling of Adsorption Isotherms and Kinetics of Reactive Dye from Aqueous Solution by Peanut Hull. Chem Eng J: 2011; 168: 1234-1240.

[5] Gong R, Ding Y, Li M, Yang C, Liu H, Sun Y. Utilization of Powdered Peanut Hull as Biosorbent for Removal of Anionic Dyes from Aqueous Solution. Dyes Pigments: 2005; 64: 187-192.

[6] Kumar KV. Optimum Sorption Isotherm by Linear and Non-Linear Methods for Malachite Green Onto Lemon Peel. Dyes Pigments: 2007; 74: 595-597.

[7] Doulati Ardejani F, Badii K, Yousefi Limaee N, Mahmoodi NM, Arami M, Shafaei SZ, Mirhabibi AR. Numerical Modelling and Laboratory Studies on the Removal of Direct Red 23 and Direct Red 80 Dyes from Textile Effluents using Orange Peel, a Low-Cost Adsorbent. Dyes Pigments: 2007; 73: 178-185.

[8] Han R, Ding D, Xu Y, Zou W, Wang Y, Li Y, Zou L. Use of Rice Husk for the Adsorption of Congo Red from Aqueous Solution in Column Mode. Bioresource Technol: 2008; 99: 2938-2946.

[9] Safa Y, Bhatti HN. Biosorption of Direct Red-31 and Direct Orange-26 Dyes by Rice Husk: Application of Factorial Design Analysis. Chem Eng Res Des: 2011; 89: 2566-2574.

[10] Khatibzadeh M, Mohseni M, Moradian S. Dye Uptake and Thermal Behavior of Fibre Grade PET Containing Boltorn H40 as a Nanomaterial. Journal of Fiber Bioengineering and Informatics: 2012; 5: 455-464.

[11] Yoshida H, Okamoto A, Kataoka T. Adsorption of Acid Dye on Cross-Linked Chitosan Fibers: Equilibria. Chem Eng J: 1993; 48: 2267-2272.

[12] Kyzas GZ, Lazaridis NK. Reactive and Basic Dyes Removal by Sorption Onto Chitosan Derivatives. J Colloid Interf Sci: 2009; 331: 32-39.

[13] Wu F, Tseng R, Juang R. Comparative Adsorption of Metal and Dye on Flake- and Bead-Types of Chitosans Prepared from Fishery Wastes. J. Hazard. Mater.: 2000; 73: 63-75.

[14] Wang H, Zheng XW, Su JQ, Tian Y, Xiong XJ, Zheng TL. Biological Decolorization of the Reactive Dyes Reactive Black 5 by a Novel Isolated Bacterial Strain *Enterobacter sp.* EC3. J Hazard Mater: 2009; 171: 654-659.

[15] Moosvi S, Kher X, Madamwar D. Isolation, Characterization and Decolorization of Textile Dyes by a Mixed Bacterial Consortium JW-2. Dyes Pigments: 2007; 74: 723-729.

[16] Asad S, Amoozegar MA, Pourbabaee AA, Sarbolouki MN, Dastgheib SMM. Decolorization of Textile Azo Dyes by Newly Isolated Halophilic and Halotolerant Bacteria. Bioresource Technol: 2007; 98: 2082-2088.

[17] Sanlier SH, Ak G, Yilmaz H, Ozbakir G, Cagliyan O. Removal of Textile Dye, Direct Red 23, with Glutaraldehyde Cross-Linked Magnetic Chitosan Beads. Preparative Biochemistry and Biotechnology: 2013; 43: 163-176.

[18] El-Reash YG, Otto M, Kenawy IM, Ouf AM. Adsorption of Cr(VI) and as(V) Ions by Modified Magnetic Chitosan Chelating Resin. Int J Biol Macromol: 2011; 49: 513-522.

[19] Zhou L, Liu Z, Liu J, Huang Q. Adsorption of Hg(II) from Aqueous Solution by Ethylenediamine-Modified Magnetic Crosslinking Chitosan Microspheres. Desalination: 2010; 258: 41-47.

[20] Shen C, Song S, Zang L, Kang X, Wen Y, Liu W, Fu L. Efficient Removal of Dyes in Water using Chitosan Microsphere Supported Cobalt (II) Tetrasulfophthalocyanine with H_2O_2. J Hazard Mater: 2010; 177: 560-566.

[21] Blackburn RS. Natural Polysaccharides and their Interactions with Dye Molecules: Applications in Effluent Treatment. Environ Sci Technol: 2004; 38: 4905.

[22] Sakkayawong N, Thiravetyan P, Nakbanpote W. Adsorption Mechanism of Synthetic Reactive Dye Wastewater by Chitosan. J Colloid Interf Sci: 2005; 286: 36-42.

[23] Saleem M, Pirzada T, Qadeer R. Sorption of Acid Violet 17 and Direct Red 80 Dyes on Cotton Fiber from Aqueous Solutions. Colloid Surface A: 2007; 292: 246-250.

[24] Cestari AR, Vieira EFS, Dos Santos, Aline G. P., Mota JA, De Almeida VP. Adsorption of Anionic Dyes on Chitosan Beads. 1. the Influence of the Chemical Structures of Dyes and Temperature on the Adsorption Kinetics. J Colloid Interf Sci: 2004; 280: 380.

[25] Mazengarb S, Roberts GAF. Studies on the Diffusion of Direct Dyes in Chitosan Film. Prog. Chem. App. Chitin Derivat.: 2009; 14: 25-32.

[26] Ho YS, McKay G. Sorption of Dye from Aqueous Solution by Peat. Chem Eng J: 1998; 70: 115-124.

[27] Prado AGS, Macedo JL, Dias SCL, Dias JA. Calorimetric Studies of the Association of Chitin and Chitosan with Sodium Dodecyl Sulfate. Colloid Surface B: 2004; 35: 23-27.

[28] Chiou MS, Li HY. Adsorption Behavior of Reactive Dye in Aqueous Solution on Chemical Cross-Linked Chitosan Beads. Chemosphere: 2003; 50: 1095-1105.

[29] McKay G, Blair HS, Gardner JR. Adsorption of Dyes on Chitin. I. Equilibrium Studies. J Appl Ploym Sci: 1982; 27: 3043-3057.

[30] Copello GJ, Mebert AM, Raineri M, Pesenti MP, Diaz LE. Removal of Dyes from Water using Chitosan hydrogel/SiO_2 and Chitin hydrogel/SiO_2 Hybrid Materials obtained by the sol–gel Method. J Hazard Mater: 2011; 186: 932-939.

[31] Ghobadi J, Arami M, Bahrami H, Mahmoodi NM. Modification of Carbon Nanotubes with Cationic Surfactant and its Application for Removal of Direct Dyes. Desalination and Water Treatment: 2013.

[32] Mahmoodi NM, Maghsoudi A, Najafi F, Jalili M, Kharrati H. Primary–secondary Amino Silica Nanoparticle: Synthesis and Dye Removal from Binary System. Desalination and Water Treatment: 2013.

[33] Julieta de Jesus da Silveirea Neta, Costa Moreira G, Da Silva CJ, Reis C, Reis EL. Use of Polyurethane Foams for the Removal of the Direct Red 80 and Reactive Blue 21 Dyes in Aqueous Medium. Desalination: 2011; 281: 55-60.

[34] Mahmoodi NM, Hayati B, Bahrami H, Arami M. Dye Adsorption and Desorption Properties of *Mentha Pulegium* in Single and Binary Systems. J Appl Polym Sci: 2011; 122: 1489-1499.

[35] Kousha M, Daneshvar E, Esmaeili AR, Zilouei H, Karimi K. Biosorption of Toxic Acidic dye–Acid Blue 25, by Aquatic Plants. Desalination and Water Treatment: 2013.

[36] Mahmoodi N. Synthesis of Amine-Functionalized Magnetic Ferrite Nanoparticle and its Dye Removal Ability. J.Environ.Eng.: 2013; 139: 1382-1390.

[37] Aguayo-Villarreal IA, Ramírez-Montoya LA, Hernández-Montoya V, Bonilla-Petriciolet A, Montes-Morán MA, Ramírez-López EM. Sorption Mechanism of Anionic Dyes on Pecan Nut Shells (*Carya Illinoinensis*) using Batch and Continuous Systems. Industrial Crops and Products: 2013; 48: 89-97.

[38] Han Z, Zhu Z, Wu D, Wu J, Liu Y. Adsorption Kinetics and Thermodynamics of Acid Blue 25 and Methylene Blue Dye Solutions on Natural Sepiolite. Synthesis and Reactivity in Inorganic, Metal-Organic, and Nano-Metal Chemistry: 2014; 44: 140-147.

[39] Daneshvar E, Kousha M, Sohrabi MS, Khataee A, Converti A. Biosorption of Three Acid Dyes by the Brown Macroalga *Stoechospermum Marginatum*: Isotherm, Kinetic and Thermodynamic Studies. Chem.Eng.J.: 2012; 195–196: 297-306.

[40] Hanafiah MAKM, Ngah WSW, Zolkafly SH, Teong LC, Majid ZAA. Acid Blue 25 Adsorption on Base Treated Shorea Dasyphylla Sawdust: Kinetic, Isotherm, Thermodynamic and Spectroscopic Analysis. Journal of Environmental Sciences: 2012; 24: 261-268.